arXiv:0911.2577v2 [hep-lat] 19 Apr 2010

The deconfinement transition of finite density QCD with heavy quarks from strong coupling series

Jens Langelage and Owe Philipsen

Institut für Theoretische Physik, Westfälische Wilhelms-Universität Münster, 48149 Münster, Germany

Abstract

Starting from Wilson's action, we calculate strong coupling series for the Polyakov loop susceptibility in lattice gauge theories for various small N_τ in the thermodynamic limit. Analysing the series with Padé approximants, we estimate critical couplings and exponents for the deconfinement phase transition. For $SU(2)$ pure gauge theory our results agree with those from Monte-Carlo simulations within errors, which for the coarser $N_\tau = 1, 2$ lattices are at the percent level. For QCD we include dynamical fermions via a hopping parameter expansion. On a $N_\tau = 1$ lattice with $N_f = 1, 2, 3$, we locate the second order critical point where the deconfinement transition turns into a crossover. We furthermore determine the behaviour of the critical parameters with finite chemical potential and find the first order region to shrink with growing μ. Our series moreover correctly reflects the known $Z(N)$ transition at imaginary chemical potential.

1   Introduction

Lattice Monte Carlo studies of the QCD phase diagram at finite temperature are still difficult for realistic quark masses, and at finite baryon density are beset by the sign-problem. Despite the progress made in the last few years in circumventing these obstacles, such calculations still suffer severe restrictions. In particular, presently available methods are reliable only for small quark chemical potentials, $\mu \lesssim T$ [1]. These difficulties motivate the search for alternative ways to learn about the phase diagram. A popular choice is to consider lattice QCD in the strong coupling limit and to study its phase diagram either by analytic mean field methods [2] or indeed by Monte Carlo evaluation of the strongly coupled theory [3],[4], since the sign problem in this case is much milder. In the early days of lattice gauge theory, strong coupling expansions for zero temperature Yang-Mills theory have led to some analytical insights into field theories on a lattice ([5],[6] and [7] for a review). They have also been used to investigate finite temperature effects [8]-[13] with reasonable qualitative predictions, but mostly using the crude approximation of neglecting spatial plaquettes altogether, cf. [14] and references therein for a review of early investigations. However, the strong coupling limit is far from the physical continuum theory and the lessons learned in this way are qualitative at best. There have also been attempts to go beyond the strong coupling limit [15]-[19], mostly in mean field theory.

In this paper we address the question whether it is possible to make predictions for the location and nature of the deconfinement phase transition more quantitative by taking corrections into account, and we can answer in the affirmative. In previous work [20] we have already shown for $SU(2)$ Yang-Mills theory that it is quite possible to include spatial plaquettes and to obtain series of several orders. For lattices with temporal extent $N_\tau = 1 - 4$, this lead to satisfactory quantitative results for the equation of state up to the phase transition region. However, while the determination of the critical parameters was consistent with Monte Carlo results and universality arguments, it remained rather imprecise quantitatively. Here we considerably improve on this by using the Polyakov loop susceptibility as an observable, rather than the free energy. At a second order phase transition in infinite volume, this observable develops a singularity which is well modelled by Padé approximants to its series expansion, thus allowing to extract the critical coupling and exponent in satisfactory agreement with numerical results from [21],[22],[23].

After a successful test of our method for $SU(2)$ Yang-Mills theory, we study the case of $SU(3)$ QCD with Wilson quarks by a combined strong coupling and hopping parameter expansion, which converges for sufficiently heavy quarks. In the infinite
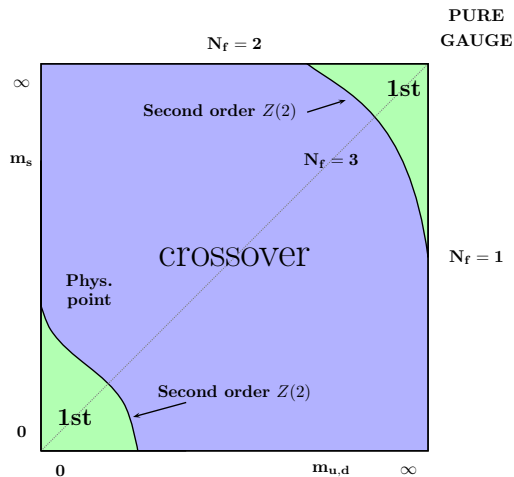
Figure 1: Schematic overview of the $N_f = 2+1$ QCD phase diagram. Here we compute the critical line for heavy quarks.

quark mass limit, QCD is known to display a first order phase transition which weakens as quark masses are lowered, see Fig. 1. The location of the critical quark mass, where the transition disappears at a second order critical point, has been studied for $N_f = 1$ by a combination of numerical simulations of QCD and the 3d 3-state Potts model [24, 25], which is the appropriate effective theory for the critical transition. These works also established the 3d Ising universality of the boundary line. Our methods allow for a determination of the critical quark mass for $N_f = 1, 2, 3$, as well as the dependence of the critical quark mass on quark chemical potential. We find that the critical mass grows with increasing chemical potential, in accord with a Monte Carlo study in the Potts model with finite chemical potential [26]. However, our result is the first based on full QCD beyond mean field theory.

2 Phase transitions from strong coupling series

2.1 Notation and formalism

We work on a $(3+1)$-dimensional hypercubic lattice with lattice spacing a and infinite spatial volume. The temporal lattice extent N_τ is kept finite, which in combination with (anti-)periodic boundary conditions for (fermionic) bosonic fields generates a non-vanishing physical temperature,

$$T = \frac{1}{N_\tau a} \ . \tag{1}$$

Using Wilson's gauge action for $SU(N)$, the partition function reads

$$Z = \int [dU] \exp\left(-S_g\right) = \int [dU] \prod_p \exp\left[\frac{\beta}{2N}\left(\operatorname{tr} U_p + \operatorname{tr} U_p^\dagger\right)\right]. \tag{2}$$

In order to locate the phase transition we consider the Polyakov loop susceptibility

$$\chi_L = V\left(\langle L^2\rangle - \langle L\rangle^2\right), \tag{3}$$

where we have defined the Polyakov loop $L_\mathbf{x}$ and its spatial average L as

$$L_\mathbf{x} = \operatorname{tr} W_\mathbf{x} = \operatorname{tr} \prod_{\tau=1}^{N_\tau} U_0(\mathbf{x}, \tau), \tag{4}$$

$$L = \frac{1}{V}\sum_\mathbf{x}\left(L_\mathbf{x} + L_\mathbf{x}^\dagger\right) \qquad SU(N \geq 3)$$

$$L = \frac{1}{V}\sum_\mathbf{x} L_\mathbf{x} \qquad\qquad SU(2). \tag{5}$$

If we couple the Polyakov loop to an external source J in the action[1],

$$-S(J) = \frac{\beta}{2N}\sum_p\left(\operatorname{tr} U_p + \operatorname{tr} U_p^\dagger\right) + J\sum_\mathbf{x}\left(L_\mathbf{x} + L_\mathbf{x}^\dagger\right), \tag{6}$$

we can express the susceptibility as

$$\chi_L = \frac{1}{V}\frac{\partial^2}{\partial J^2}\ln Z(J)\bigg|_{J=0}. \tag{7}$$

In order to obtain a strong coupling series for Eq. (7), we expand the partition function

$$Z(J) = \int [dU]\left[\prod_p \exp\left(\frac{\beta}{2N}\left(\operatorname{tr} U_p + \operatorname{tr} U_p^\dagger\right)\right)\right]\left[\prod_\mathbf{x} \exp\left(J\left(\operatorname{tr} W_\mathbf{x} + \operatorname{tr} W_\mathbf{x}^\dagger\right)\right)\right] \tag{8}$$

in terms of characters

$$\exp\left(\frac{\beta}{2N}\left(\operatorname{tr} U_p + \operatorname{tr} U_p^\dagger\right)\right) = \left[1 + \sum_{r\neq 0} d_r a_r\left(\beta\right)\chi_r(U_p)\right] \tag{9}$$

$$\exp\left(J\left(\operatorname{tr} W_\mathbf{x} + \operatorname{tr} W_\mathbf{x}^\dagger\right)\right) = c_0(J)\left[1 + \sum_{r\neq 0} b_r(J)\chi_r(W_\mathbf{x})\right]. \tag{10}$$

---

[1] For $SU(3)$ we have chosen L as the real part of the Polyakov loop, so we get a real action with only one real source J
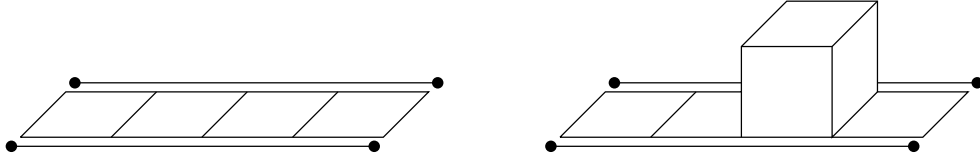
Figure 2: Examples for $N_\tau = 4$. Left: Two Polyakov loops and N_τ plaquettes wind around the temporal dimension. Right: The first correction with additional plaquettes.

We have neglected the prefactor $c_0(\beta)$ of the trivial representation because it does not depend on J and vanishes in Eq. (7). As usual in strong coupling expansions, we will use the coefficient $u = a_f$ of the fundamental representation as expansion parameter.

In the case of $SU(2)$ we have no complex conjugate representations and the partition function reads

$$Z(J) = \int [dU] \left[\prod_p \exp \left(\frac{\beta}{2} \operatorname{tr} U_p \right) \right] \left[\prod_{\mathbf{x}} \exp \left(J \operatorname{tr} W_{\mathbf{x}} \right) \right]. \tag{11}$$

Furthermore, there are closed form expressions for the expansion coefficients in this case,

$$a_j(\beta) = \frac{I_{2j+1}(\beta)}{I_1(\beta)}, \tag{12}$$

$$b_j(J) = \frac{d_j I_{2j+1}(2J)}{I_1(2J)}, \tag{13}$$

$$c_0(J) = \frac{I_1(2J)}{J}. \tag{14}$$

Applying a cluster expansion as described in [27], the logarithm of the partition function can be represented as a sum of graphs $\Phi(C)$

$$\frac{1}{V} \ln Z(J) = \ln c_0(J) + \sum_C \Phi(C). \tag{15}$$

The sum is over all clusters C of connected polymers, see [20] for details. The leading order, i.e. the strong coupling limit $\beta = 0$, is obtained by neglecting all graphs giving the trivial result

$$\chi_L = \frac{\partial^2}{\partial J^2} \ln c_0(J) \bigg|_{J=0} = 1 + \mathcal{O}(u^{N_\tau}) \qquad SU(2)$$

$$\chi_L = \frac{\partial^2}{\partial J^2} \ln c_0(J) \bigg|_{J=0} = 2 + \mathcal{O}(u^{N_\tau}) \qquad SU(N \geq 3). \tag{16}$$

In case of $SU(N \geq 3)$ the factor of 2 accounts for both fundamental representations.

4

The first graph with a non-trivial u-dependence is shown in Fig. 2, together with the leading correction graph. The left and the right boundaries of these graphs are meant to be identified due to the periodic boundary conditions. To calculate the contribution of these graphs, we employ the group integration formula

$$\int dU \chi_r(U) \chi_s(U^\dagger) = \frac{\delta_{rs}}{d_r}, \tag{17}$$

and get

$$
\begin{aligned}
\Phi_0 &= 3u^{N_\tau} \left(b_{1/2}(J)\right)^2 & SU(2), \\
\Phi_0 &= 6u^{N_\tau} \left(b_f(J)\right)^2 & SU(N \geq 3),
\end{aligned}
\tag{18}
$$

for the leading non-trivial order and

$$
\begin{aligned}
\Phi_1 &= 12 N_\tau u^{N_\tau+4} \left(b_{1/2}(J)\right)^2 & SU(2), \\
\Phi_1 &= 24 N_\tau u^{N_\tau+4} \left(b_f(J)\right)^2 & SU(N \geq 3).
\end{aligned}
\tag{19}
$$

for the first correction.

2.2 Graphical expansion

From Eq. (7) it is obvious that we solely have to take into account graphs which contribute to order J^2. This means that only graphs with two Polyakov loops in the fundamental or one loop in the adjoint representation are allowed. For the first possibility, the loops have to be on different lattice sites. The generation of contributing graphs is not uniform and we distinguish between small, intermediate and large N_τ.

Large N_τ: Large N_τ receive only contributions from nearest-neighbour Polyakov loops as shown in Fig. 2, and corrections from adding plaquettes. Of course, this statement is only true for large enough N_τ if we calculate to some fixed order in u.

Small N_τ: The smallest possible N_τ is 1. Typical graphs are shown in Fig. 3. These graphs are meant to be spatial projections of graphs like in Fig. 2 (left). In higher orders we get contributions from additional spatial plaquettes, e.g. by filling the cross-section of the self-avoiding polygons, but these contributions are small compared to the increasing number of self-avoiding walks.

Intermediate N_τ: For intermediate N_τ (=2,3,4...) we have to take into account graphs of both types. There are also some other corrections as shown in Fig. 4. Thus these N_τ are the most labour-intensive ones.
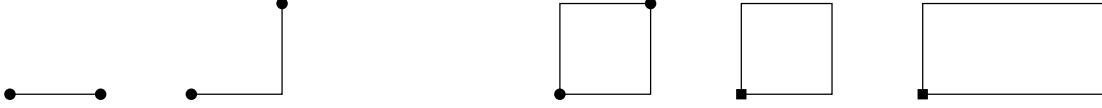
Figure 3: Left: Self avoiding walks with two fundamental Polyakov loops. Right: Self avoiding polygons with one adjoint or two fundamental Polyakov loop.
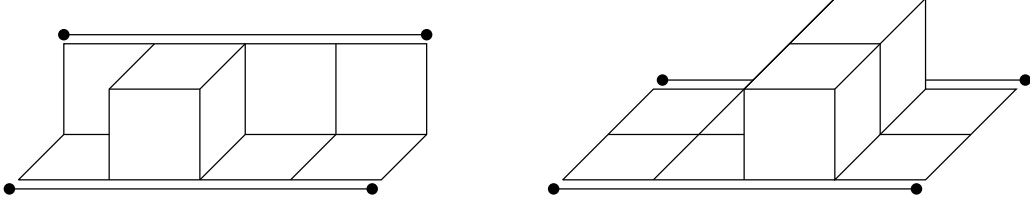

Figure 4: Examples of corrections to self avoiding walks of length $L = 2$ and $N_\tau = 4$.

2.3 Series analysis and phase transitions

Strong coupling expansions have a finite radius of convergence. Expanding about $\beta = 0$, a true deconfinement phase transition at some critical value of β_c clearly represents an upper bound on the convergence radius, i.e. strong coupling analyses are limited to the confined region. Nevertheless, knowledge of the series coefficients allows us to estimate the location of a singularity along the real β-axis. Our analysis is well suited to detect second order phase transitions and exploits the fact that the Polyakov loop susceptibility in this case diverges with a critical exponent. Near a critical coupling the Polyakov loop susceptibility and its logarithmic derivative behave like

$$\chi_L \sim \frac{1}{(u_c - u)^\gamma} \ , \qquad\qquad D_\chi(u) \equiv \frac{d}{du}\ln{(\chi_L)} \sim \frac{\gamma}{(u_c - u)}. \qquad (20)$$

From our series expansions we know $D_\chi(u)$ as a polynomial in u and can model its pole-like singularity by Padé approximants

$$[L, M](u) \equiv \frac{a_0 + a_1 u + \cdots + a_L u^L}{1 + b_1 u + \cdots + b_M u^M}. \qquad (21)$$

In order to uniquely determine the coefficients a_i, b_i, it is necessary to have $L+M \leq N$, if N represents the highest available order of the expansion. In this way a $[L, M]$ approximant is correct up to but not including $\mathcal{O}(u^{L+M+1})$ and larger approximants represent more expansion coefficients than smaller ones. In particular, the critical coupling u_c is given as the real positive zero of the denominator closest to the origin, the critical exponent γ is obtained from the corresponding residuum.

The analysis can be made more powerful if either independent results for the critical couplings are available, or the universality class of the transition is known. In the first

case, it is possible to get better estimates for the critical exponents via

$$(u_c - u)D_\chi(u) = \gamma + \mathcal{O}(u_c - u), \tag{22}$$

which is the more precise the better we know u_c. In order to do so, we calculate Padé approximants to the series expansion of $(u_c - u)D_\chi(u)$ and evaluate them at the known critical coupling u_c. In the same way we can use a known value γ to get more accurate estimates for the critical coupling

$$(\chi_L)^{\frac{1}{\gamma}} \sim \frac{1}{(u_c - u)} . \tag{23}$$

Here we calculate Padé approximants to $(\chi_L)^{\frac{1}{\gamma}}$ and solve for zeros of the denominator, as this quantity has a simple pole at the critical coupling. For a more detailed discussion of these topics, see [28].

3 $SU(2)$ Yang-Mills

3.1 Results for the series

We first apply our analysis method to $SU(2)$ pure gauge theory, where we have reasonably long series for $N_\tau = 1 - 4$ and where accurate Monte Carlo data are available for comparison. We obtain the following strong coupling series for $\chi_L(N_\tau, u)$:

$$
\begin{aligned}
\chi_L(1, u) &= 1 + 6\,u + 30\,u^2 + 150\,u^3 + 738\,u^4 + 3622\,u^5 + \frac{52982}{3}u^6 + \\
&\quad + \frac{773434}{9}u^7 + \frac{11239612}{27}u^8 + \mathcal{O}\left(u^9\right), \\
\chi_L(2, u) &= 1 + 6\,u^2 + 30\,u^4 + 222\,u^6 + 1218\,u^8 + \frac{24602}{3}u^{10} + \mathcal{O}\left(u^{12}\right), \\
\chi_L(3, u) &= 1 + 6\,u^3 + 30\,u^6 + 72\,u^7 + 72\,u^8 + 78\,u^9 + 576\,u^{10} + 1776\,u^{11} + \\
&\quad + 1770\,u^{12} + \mathcal{O}\left(u^{13}\right), \\
\chi_L(4, u) &= 1 + 6\,u^4 + 126\,u^8 + 48\,u^{10} + 2830\,u^{12} + \frac{91808}{135}u^{14} + \mathcal{O}\left(u^{16}\right). \tag{24}
\end{aligned}
$$

$N_\tau = 1$ corresponds to the largest lattice spacing and thus to the largest bare coupling at the deconfinement transition. Hence, our series shows the best convergence behaviour in this case.

Padé	u_c	β_c	γ
$[5,2]$	0.21055	0.86825	1.167
$[3,3]$	0.20967	0.86439	1.138
$[4,2]$	0.20957	0.86396	1.146
$[2,4]$	0.20987	0.86527	1.135
$[3,2]$	0.20927	0.86264	1.126
$[2,2]$	0.20820	0.85796	1.102
Mean	0.2095(12)	0.864(5)	1.14(3)

Table 1: Critical coupling and exponent for $N_\tau = 1$, estimated from different Padé approximants.

3.2 The critical parameters

We consider only Padés $[L, M]$ with $L, M > 2$ in order to have large enough polynomials in both numerator and denominator. So-called defective approximants with an adjacent zero-pole pair, indicated by a small residuum (we chose $Res < 0.003$ to be defective), are also ignored. By doing so we obtain estimates for the critical parameters as shown in Table 1. In the last line we have averaged over the estimates from different Padés in order to quantify the systematic error associated with the choice of a particular approximant. Note that the quoted error is estimated as $(\beta_c^{max} - \beta_c^{min})/2$, and similarly for the exponent. It is only due to the scatter in the singularity structure of different Padé approximants and does not include the error from the truncation of the series, i.e. it likely underestimates the true error.

Our result for a $N_\tau = 1$ lattice then is $\beta_c = 0.864(5), \gamma = 1.14(3)$. There exist different values for the critical coupling from Monte Carlo simulations in the literature: $\beta_c = 0.8730(2)$ from [21] and the more recent $\beta_c = 0.85997(10)$ or $0.86226(6)$ from [23]. At first sight our results appear to favour one of the latter, but with a critical exponent deviating about 10% from universality. While the Padé approximants accumulate a pole and thus definitely predict a second order phase transition, the residuum is somewhat below the value $\gamma_I = 1.2373(2)$ [29] for a 3d Ising transition. Note however the upward trend in the critical coupling as well as in the exponent with increasing order $L + M$ of the approximants in Table 1. This indicates that the results are not yet fully stable and the exponent should reach the Ising value with longer series.

It is apparent that we have gained considerable accuracy compared to previous work using the free energy and its derivatives as observables [20], which gives $\beta_c = 0.92(15), \alpha = 0.063(38)$ ($\alpha = 0.1096(5)$ for 3d Ising [29]). The reason for this improve-

Padé	u_c	β_c
[6, 2]	0.21221	0.87553
[4, 3]	0.21159	0.87281
[2, 5]	0.21138	0.87189
[3, 3]	0.21229	0.87588
[2, 4]	0.21238	0.87628
[4, 2]	0.21279	0.87808
[3, 2]	0.20986	0.86523
[2, 3]	0.21464	0.88621
[2, 2]	0.21495	0.88757

Padé	γ_1	γ_2
[3, 4]	1.1250	1.2378
[4, 3]	1.1244	1.2331
[2, 5]	1.1246	1.2157
[5, 2]	1.1244	1.2208
[3, 3]	1.1225	1.2579
[2, 4]	1.1236	1.2661
[4, 2]	1.1244	1.2950
[3, 2]	1.1240	1.2308
[2, 3]	1.1238	1.2215

Table 2: Biased critical couplings and exponents for $N_\tau = 1$.

ment is twofold: the Polyakov loop susceptibility permits an easier evaluation of more coefficents, e.g. by featuring both even and odd powers of u, and the series itself comes with only positive coefficients and is better behaved than that for the free energy.

It is now interesting to explore how one can combine Monte Carlo and series results. Thus we consider biased estimates, which should be more accurate. Using $\gamma_I = 1.237$, we get the results shown in Table 2. We calculate the average of β_c to be $\overline{\beta_c} = 0.877(11)$ using all Padés and $\overline{\beta_c} = 0.875(3)$ using only the three highest orders which behave more smoothly. Despite the fact that the total error is underestimated, both estimates are consistent with the Monte Carlo result of [21].

In order to obtain the biased critical exponent, we used the values $\beta_1 = 0.86226$ and $\beta_2 = 0.873$. The former gives a mean critical exponent of $\overline{\gamma_1} = 1.124(1)$ and the latter $\overline{\gamma_2} = 1.24(4)$. Although the first result is much more stable, it is the second one which is consistent with universality. Hence we conclude that it is the value $\beta_c = 0.8730(2)$ of [21], which is supported by our series expansions.

For intermediate N_τ our results become less precise the larger we choose N_τ. This is to be expected since β_c grows on finer lattices and we are leaving the strong coupling regime. Thus we only give our biased estimates, using the Monte Carlo results $\beta_c(N_\tau = 2) = 1.87348, \beta_c(N_\tau = 3) = 2.1768, \beta_c(N_\tau = 4) = 2.2993$ [22],[23] and $\gamma_I = 1.237$. We summarise our results in Table 3 and observe that the predicted quantities are fully consistent with Monte Carlo results and universality.

N_τ	γ_I	$\overline{\gamma}$	No. of Padés	β_c^{MC}	$\overline{\beta}_c$	No. of Padés
2	1.237	1.21(2)	5	1.87348(2)	1.87(1)	6
3	1.237	1.29(18)	2	2.1768(30)	2.13(4)	6
4	1.237	1.22(20)	3	2.2993(3)	2.23(11)	7

Table 3: Comparison of our findings, $\overline{\gamma}, \overline{\beta}_c$, with the values from universality and simulations.

4 $SU(3)$ and QCD

For $SU(3)$ Yang-Mills theory, there is a first order phase transition, i.e. the correlation length remains finite even at the critical temperature, spoiling our analysis method which requires scaling behaviour. We therefore introduce heavy dynamical quarks, which have a critical mass m_c where the transition turns second order, cf. Fig. 1. It is this point which we now try to locate.

4.1 Combined strong coupling and hopping expansion

We introduce dynamical quarks in leading order hopping parameter expansion (see [27] for details), where the quark part of the action reads

$$S_q = \sum_l \frac{\kappa^l}{l} \operatorname{tr} M[U]^l, \qquad \kappa = \frac{1}{2m + 8}, \tag{25}$$

m is the quark mass and $M[U]$ the quark hopping matrix

$$M[U]_{yx} = \sum_\mu \delta_{y,x+\hat{\mu}}(1 + \gamma_\mu)U_{x\mu}. \tag{26}$$

The sum in Eq. (25) extends over all closed paths on the lattice. For small temporal lattice sizes and finite temperature the leading order hopping expansion term is just the Polyakov loop $\operatorname{tr} W_{\mathbf{x}}$. Chemical potential is introduced in the usual way as factors $\exp(\pm\mu)$ to the temporal link variables [30]. The effective quark part of the action for small temporal lattice extents then reads

$$-S_q^{eff} = \sum_{\mathbf{x}} \left[h(\kappa)e^\mu \operatorname{tr} W_{\mathbf{x}} + h(\kappa)e^{-\mu} \operatorname{tr} W_{\mathbf{x}}^\dagger \right], \tag{27}$$

where the relative minus sign compared to Eq. (25) is due to the antiperiodic boundary conditions for fermions. The parameter $h(\kappa)$ depends on the hopping parameter κ and

the number of degenerate quark flavours N_f via

$$h(\kappa) = 2N_f(2\kappa)^{N_\tau}. \tag{28}$$

For $\mu \neq 0$ the action is complex.

Introducing Polyakov loop source terms J and putting everything together, we obtain the following partition function

$$
\begin{aligned}
Z &= \int [dU] \exp\left[\frac{\beta}{6}\sum_p\left(\mathrm{tr}U_p + \mathrm{tr}U_p^\dagger\right)\right. \\
&\quad + \left.\sum_{\mathbf{x}}\left\{\left[he^\mu + J\right]\mathrm{tr}\,W_{\mathbf{x}} + \left[he^{-\mu} + J\right]\mathrm{tr}\,W_{\mathbf{x}}^\dagger\right\}\right].
\end{aligned}
\tag{29}
$$

Now we can proceed in the same way as in case of $SU(2)$ and rewrite the partition function with two different character expansions and omit the factor $c_0(\beta)$

$$
\begin{aligned}
Z &= \int [dU] \prod_p\left[1 + \sum_{r\neq 0} d_r a_r(\beta)\chi_r(U_p)\right] \\
&\quad \times \prod_{\mathbf{x}} c_0(h, \mu, J)\left[1 + \sum_{r\neq 0} b_r(h, \mu, J)\chi_r(W_{\mathbf{x}})\right].
\end{aligned}
\tag{30}
$$

Note that for non-vanishing chemical potential μ the expansion parameters $b_r(h, \mu, J)$ are different for complex conjugate representations r and $\bar{r}$ and related via

$$b_r(h, \mu, J) = b_{\bar{r}}(h, -\mu, J). \tag{31}$$

The expansion coefficients itself can be expressed as series expansions, e.g.

$$
\begin{aligned}
u \equiv a_f(\beta) &= \frac{1}{18}\beta + \dots, \\
c_0(h, \mu, J) &= 1 + \left(he^\mu + J\right)\left(he^{-\mu} + J\right) + \dots, \\
b_f(h, \mu, J) &= he^\mu + J + \dots.
\end{aligned}
\tag{32}
$$

In order to get the proper series expansion we now have to draw all possible diagrams to a given order in u and the number of Polyakov loops l. In contrast to our $SU(2)$ calculation we have to take into account not only the graphs with two Polyakov loop source terms, but all graphs with contributions of the order $J^2 h^m$, since these give finite results after differentiating twice with respect to J and setting $J = 0$. Some examples of graphs for the case $N_\tau = 1$ are given in Fig. 5. An important fact is that for a given order in u, there is only a finite number of graphs. For the order u^n, we can have only graphs fulfilling $l \leq 2n$, as inspection of the series shows. Additional terms in the hopping expansion will modify the b_r's and rapidly increase the number of relevant graphs.
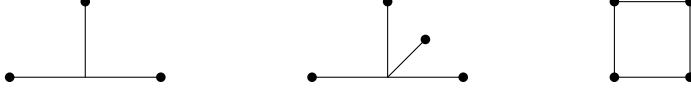
Figure 5: Examples of terms with a larger number of Polyakov loop source terms.

4.2 Result for the series

We have derived the series expansion of the Polyakov loop susceptibility up to orders $u^n h^m$, with $n + m \leq 6$. The result for the $N_\tau = 1$ series, arranged in increasing orders of u, reads

$$
\begin{aligned}
\chi_L(u, h) &= \left[1 + ch + \left(-\frac{4}{3}c^3 + \frac{1}{2}c \right) h^3 + \left(-\frac{5}{3}c^4 + \frac{4}{3}c^2 - \frac{7}{24} \right) h^4 \right. \\
&\quad \left. + \left(\frac{2}{15}c^5 + \frac{1}{3}c^3 - \frac{1}{8}c \right) h^5 + \left(\frac{28}{15}c^6 - \frac{7}{5}c^4 - \frac{7}{120}c^2 + \frac{119}{720} \right) h^6 \right] \\
&\quad + \left[6 + 18ch + \left(6c^2 + 3 \right) h^2 + \left(-40c^3 + 15c \right) h^3 \right. \\
&\quad \left. + \left(-90c^4 + 66c^2 - \frac{69}{4} \right) h^4 + \left(-\frac{32}{5}c^5 - 8c^3 + 6c \right) h^5 \right] u \\
&\quad + \left[30 + 180ch + \left(144c^2 + 72 \right) h^2 + \left(-760c^3 + 285c \right) h^3 \right. \\
&\quad \left. + \left(-\frac{5985}{2}c^4 + \frac{8985}{4}c^2 - \frac{4485}{8} \right) h^4 \right] u^2 \\
&\quad + \left[150 + 1470ch + \left(\frac{4113}{2}c^2 + \frac{4113}{4} \right) h^2 \right. \\
&\quad \left. + \left(-6856c^3 + 2571c \right) h^3 \right] u^3 \\
&\quad + \left[786 + 10752ch + \left(\frac{1131747}{32}c^2 + \frac{1088547}{64} \right) \right] u^4 \\
&\quad + \left[4011 + 73521ch \right] u^5 + \frac{152247}{8} u^6,
\end{aligned}
\tag{33}
$$

where we used the abbreviation $c \equiv \cosh(\mu)$. Since the only μ-dependence appears in $\cosh(\mu)$ terms, one can immediately see that the Polyakov loop susceptibility is invariant under $\mu \leftrightarrow -\mu$ as it should be according to the charge conjugation symmetry of QCD.

4.3 Critical point for $\mu = 0$

In order to locate the critical point $(\beta_c, \kappa_c)(\mu)$ we have to adjust our analysis methods to multiple variables. For a given number of flavours, the schematic phase diagram is
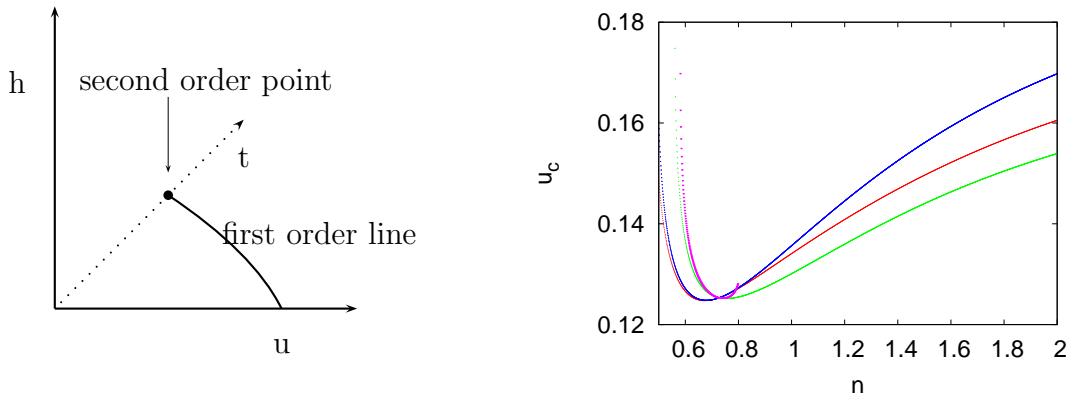
Figure 6: Left: Schematic phase diagram in the variables (u, h) of the series Eq. (33). Right: Poles of different Padé approximants (red:[1,3], blue:[0,2], green:[0,3], purple:[1:2]) accumulate for a slope parameter $n = 0.730$ at the critical point $u_c = 0.126$.

shown in Fig. 6. Our expansion is performed about $(u, h) = (0, 0)$ and we now approach the critical point along some straight line starting at the origin,

$$
\begin{aligned}
u &= n \cdot t, \\
h &= \frac{1}{n} \cdot t,
\end{aligned}
\tag{34}
$$

whose slope is tuned by n and t parametrises the distance from the critical point. We then expect a scaling behaviour

$$
\chi_L(t) \sim \frac{1}{(t_c - t)^\lambda},
\tag{35}
$$

with some critical exponent λ. The critical point is in the 3d Ising universality class, but we do not know the scaling fields and variables. The Polyakov loop in general mixes contributions from both energy-like and magnetic field-like variables. When approaching the critical point along a straight line from the origin, the larger exponent will dominate and in case of 3d Ising universality this is γ.

Our strategy now is to vary n and calculate DLog-Padés and singularities for each value. If the axis misses the critical point, there is no scaling behaviour and we expect any real poles in t, and hence in u, of the Padé approximants to be widely scattered. As the critical point is approached, these poles accumulate in a narrow window, as in our $SU(2)$ study, cf. Fig. 6. Thus, we estimate t_c as the mean value over all Padé singularities evaluated at that n for which its standard deviation is minimal. As an error estimate we take the larger one of those two values, where the standard deviation is 1.5 times its minimum. With this method we find for $\mu = 0$

$$
n = 0.730(16), \qquad \overline{t_c} = 0.172(4), \qquad \overline{\lambda} = 1.03(3).
\tag{36}
$$

13

Let us note that the standard deviations for both t and λ reach their minimum for the same slope parameter n. The critical exponent obtained with this method again underestimates γ compared to the Ising exponent. Judging from our experience with $SU(2)$, we associate this with the truncation of the strong coupling series. From Eq. (34) we obtain

$$u_c = 0.126(1), \qquad h_c = 0.236(11). \tag{37}$$

To get more accurate results, we now employ biasing with the 3d Ising exponent $\gamma = 1.237$, which leads to the improved values

$$u_c = 0.131(1) \quad \rightarrow \quad \beta_c = 2.03(2) \qquad h_c = 0.249(13). \tag{38}$$

Note that, to leading order in the hopping expansion, β_c does not depend on N_f. Inverting Eq. (28) in case of $\mu = 0$ we find

$$\kappa = \frac{1}{2} \left(\frac{h}{2N_f} \right)^{\frac{1}{N_\tau}}. \tag{39}$$

This leads to the following results for $\kappa_c(N_f)$ on a $N_\tau = 1$ lattice

$$
\begin{aligned}
N_f = 1: & \quad \kappa_c & = & \quad 0.062(4), \\
N_f = 2: & \quad \kappa_c & = & \quad 0.031(2), \\
N_f = 3: & \quad \kappa_c & = & \quad 0.021(1).
\end{aligned}
\tag{40}
$$

For these small values our leading order in the hopping expansion should be an excellent approximation. This further justifies use of the relation [9]

$$\kappa = \frac{1}{2} e^{-ma}, \tag{41}$$

which is valid for heavy quarks, to obtain the critical quark masses as

$$
\begin{aligned}
N_f = 1: & \quad m_c/T & = & \quad 2.08(7), \\
N_f = 2: & \quad m_c/T & = & \quad 2.78(7), \\
N_f = 3: & \quad m_c/T & = & \quad 3.17(10).
\end{aligned}
\tag{42}
$$

The relative size is consistent with qualitative expectations. Since the presence of finite mass quarks weakens the first order transition, more flavours of quarks should have a stronger effect and thus a larger critical quark mass.

4.4 Critical point for $\mu \neq 0$

Next we turn on a chemical potential. Eq. (33) has already been obtained for finite chemical potential, all we have to do is to repeat the same steps to search for singularities as described in the previous analysis. Of particular interest is the movement of the critical masses m_c with μ. We have calculated this function for the case of $N_f = 3$
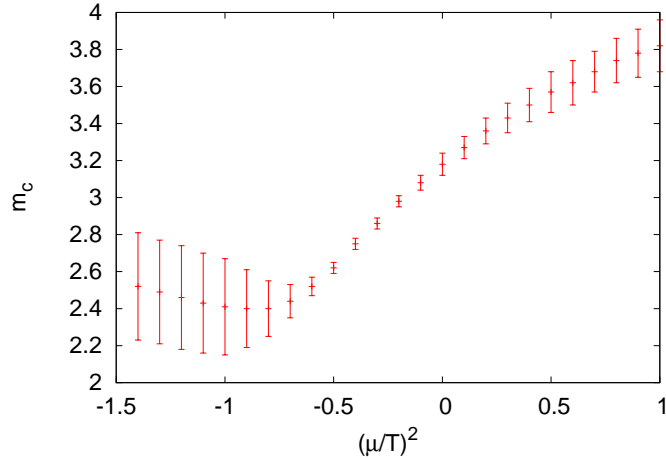

Figure 7: The critical mass $m_c(\mu^2)$ for $N_f = 3, N_\tau = 1$ as a function of real and imaginary chemical potential. Error bars are obtained with the same method as described before Eq. (36).

at several points, Fig. 7. The critical masses grow with real μ, i.e. the first order region is shrinking. For small μ we performed a fit to a low order polynomial to get a rough picture of the behaviour of the signs of the different coefficients,

$$m_c(\mu^2) = 3.18 + 0.94(1)\mu^2 - 0.34(1)\mu^4 + 0.037(18)\mu^6 + \ldots, \tag{43}$$

where the errors are those of the fitting procedure. The shrinking of the first order region, and in particular the positive curvature of the critical surface as well as the alternating signs are in accord with the findings of a Monte Carlo investigation of the Potts model [26]. To leading order hopping expansion different N_f only shift the constant term in Eq. (43).

The alternating signs indicate a convergence limiting singularity on the negative μ^2 axis, i.e. at imaginary chemical potential. Thus it is interesting to continue $m_c(\mu^2)$ also to negative values of the argument, by setting $\mu \to i\mu$. In Eq. (33), this means that c now abbreviates $\cos(\mu)$ instead of $\cosh(\mu)$. The corresponding curve is also shown in Fig. 7. We observe a minimum at about $\mu^2 \simeq -0.85$ and rapidly increasing errors with more negative μ^2. We interpret this as the point where the singularity is located.

15

This is fully consistent with the Roberge-Weiss $Z(N)$ transition point in the imaginary direction, which is known exactly to be at $\mu^2 = -\pi^2/9 \simeq -1.1$ [31].

5   Conclusions

We have explored the feasibility of calculating the critical couplings and exponents of the deconfinement transition of lattice QCD by means of analytically computed strong coupling series, using the Polyakov loop susceptibility as an observable. Our treatment is purely analytical and goes beyond mean field theory. Tables 2, 3, Eq. (42) and Fig. 7 contain our main results. For $SU(2)$ Yang-Mills theory on $N_\tau = 1 - 4$ lattices, our results are fully consistent with numerical values from Monte Carlo simulations. In the cases $N_\tau = 1, 2$ we were able to reproduce these values nearly exactly with an accuracy of a few percent, for $N_\tau = 3, 4$ the results agree within increasing error bars. For $N_\tau > 4$ the strong coupling series to the computed length becomes unpredictive, at least for our observable. A similar conclusion was drawn in [15].

In case of $SU(3)$ with heavy quarks we performed a strong coupling expansion in the effective action to leading order hopping expansion. Analysis of the $N_\tau = 1$ series allowed to extract the critical quark mass $m_c(\mu)$, for which the first order deconfinement transition goes critical before turning into a crossover. We find the first order transition region to shrink with increasing chemical potential. This is consistent with the findings from mean field theory [11] and a Monte Carlo simulation of the effective theory with the same global symmetries, the 3-state Potts model in 3 dimensions [26]. The latter is the appropriate effective model also for continuum QCD. Since our series furthermore correctly reflects the presence of the $Z(N)$ transition in the direction of imaginary chemical potential, this would suggest that the qualitative phase structure is correctly represented on lattices as coarse as $N_\tau = 1$.

We conclude that strong coupling expansions are able to provide qualitative and, on coarse lattices, quantitative information about the phase structure of lattice QCD beyond mean field theory and the strong coupling limit, which easily extend to finite baryon density. While the location of phase transitions in the parameter space is subject to renormalisation in the continuum limit, the presence of critical lines or surfaces is guaranteed by universality to survive in the continuum limit. This strongly motivates further studies to extend our analyses to finer lattices and to the light quark regime.

Acknowledgement:

References

[1] O. Philipsen, Eur. Phys. J. ST **152** (2007) 29 [arXiv:0708.1293 [hep-lat]].

[2] N. Kawamoto, K. Miura, A. Ohnishi and T. Ohnuma, Phys. Rev. D **75**, 014502 (2007) [arXiv:hep-lat/0512023].

[3] F. Karsch and K. H. Mütter, Nucl. Phys. B **313**, 541 (1989).

[4] M. Fromm and P. de Forcrand, arXiv:0811.1931 [hep-lat].

[5] K. G. Wilson, Phys. Rev. D **10** (1974) 2445.

[6] G. Münster, Nucl. Phys. B **190**, 439 (1981) [Erratum-ibid. B **200**, 536 (1982), Erratum-ibid. B **205**, 648 (1982)].

[7] J. M. Drouffe and J. B. Zuber, Phys. Rept. **102**, 1 (1983).

[8] J. Polonyi and K. Szlachanyi, Phys. Lett. B **110**, 395 (1982).

[9] F. Green and F. Karsch, Nucl. Phys. B **238**, 297 (1984).

[10] A. M. Polyakov, Phys. Lett. B **72** (1978) 477.

[11] T. Celik, T. Firat, Y. Gunduc and M. Onder, Phys. Rev. D **35**, 3958 (1987).

[12] G. Fäldt and B. Petersson, Nucl. Phys. B **265**, 197 (1986).

[13] L. Susskind, Phys. Rev. D **20**, 2610 (1979).

[14] B. Svetitsky, Phys. Rept. **132**, 1 (1986).

[15] F. Green, Nucl. Phys. B **215**, 83 (1983).

[16] M. Billo, M. Caselle, A. D'Adda and S. Panzeri, Nucl. Phys. B **472**, 163 (1996) [arXiv:hep-lat/9601020].

[17] A. Ohnishi, N. Kawamoto and K. Miura, J. Phys. G **34** (2007) S655 [arXiv:hep-lat/0701024].

[18] A. Ohnishi, K. Miura, T. Z. Nakano and N. Kawamoto, arXiv:0910.1896 [hep-lat].

[19] K. Miura, T. Z. Nakano, A. Ohnishi and N. Kawamoto, Phys. Rev. D **80**, 074034 (2009) [arXiv:0907.4245 [hep-lat]].

[20] J. Langelage, G. Münster and O. Philipsen, JHEP **0807**, 036 (2008) [arXiv:0805.1163 [hep-lat]].

[21] R. Ben-Av, H. G. Evertz, M. Marcu and S. Solomon, Phys. Rev. D **44**, 2953 (1991).

[22] J. Fingberg, U. M. Heller and F. Karsch, Nucl. Phys. B **392**, 493 (1993) [arXiv:hep-lat/9208012].

[23] A. Velytsky, Int. J. Mod. Phys. C **19**, 1079 (2008) [arXiv:0711.0748 [hep-lat]].

[24] C. Alexandrou, A. Borici, A. Feo, P. de Forcrand, A. Galli, F. Jegerlehner and T. Takaishi, Phys. Rev. D **60** (1999) 034504 [arXiv:hep-lat/9811028].

[25] F. Karsch and S. Stickan, Phys. Lett. B **488** (2000) 319 [arXiv:hep-lat/0007019].

[26] S. Kim, Ph. de Forcrand, S. Kratochvila and T. Takaishi, PoS **LAT2005**, 166 (2006) [arXiv:hep-lat/0510069].

[27] I. Montvay and G. Münster, *Cambridge, UK: Univ. Pr. (1994) 491 p. (Cambridge monographs on mathematical physics)*

[28] A. J. Guttman, in *Phase Transitions and Critical Phenomena*, Vol. 13, p.1, eds. C. Domb and J. L. Lebowitz, Academic Press, London, 1989

[29] M. Campostrini, A. Pelissetto, P. Rossi and E. Vicari, Phys. Rev. E **65**, 066127 (2002) [arXiv:cond-mat/0201180].

[30] P. Hasenfratz and F. Karsch, Phys. Lett. B **125**, 308 (1983).

[31] A. Roberge and N. Weiss, Nucl. Phys. B **275**, 734 (1986).